EmAIT

Emerging
Advances in
Integrated
Technology

Effect of Milling Time on Physical and Mechanical Properties of Ceramics Derived from the CaO-MgO-Al$_2$O$_3$-SiO$_2$ System

Hamisah Ismail[1], Hasmaliza Mohamad[1*], Rosniza Hussin[2,3]

[1]School of Materials and Mineral Resources Engineering,
 Universiti Sains Malaysia, Nibong Tebal, Penang, 14300 MALAYSIA

[2]Department of Mechanical Engineering Technology, Faculty of Engineering Technology
 Universiti Tun Hussein Onn Malaysia, Pagoh Campus, Edu Hub Pagoh, KM 1, Jalan Panchor, 84600 Johor,
 MALAYSIA

[3]Advanced Manufacturing and Materials Centre (AMMC), Faculty of Mechanical and Manufacturing Engineering,
 Universiti Tun Hussein Onn Malaysia, 86400, Parit Raja, Batu Pahat, Johor, MALAYSIA

*Corresponding Author

Abstract: This study produced ceramics powder derived from the CaO-MgO-Al$_2$O$_3$-SiO2 system using mechanical wet milling and cold pressing method. The milling time was changed between 30 min to 2 h and sintered at 950 ºC for 1 h. The pellet was performed via cold pressing in ambient temperature and pressure of 5 tonnes. The effect of milling time on the linear shrinkage, density, porosity and compressive strength of the derived from CaO-MgO-Al$_2$O$_3$-SiO$_2$ system were investigated. X-ray diffraction results demonstrated that a multi-phase of quartz and akermanite-gehlenite was obtained after sintering at 950 °C for 1 h. The results show that the increasing milling time had significantly affected the ceramics' particle size, specific surface area, phase, linear shrinkage, density, porosity, compressive strength and Young's modulus. When the milling time was raised, the density and compressive strength decreased. However, the increase in milling time increased the linear shrinkage and porosity. It was observed that the compressive strength of the pellets reached their maximum value (16.6 MPa) at a milling time of 1h and then decreased with increasing milling time.

Keywords: Milling time, CaO-MgO-Al$_2$O$_3$-SiO$_2$ system, akermanite-gehlenite, density, porosity, compressive strength

1. Introduction

Melilites are a group of minerals which form solid solutions between the end members akermanite (Ca$_2$MgSi$_2$O$_7$), gehlenite (Ca$_2$Al$_2$SiO$_7$ or C$_2$AS), soda-melilite (NaCaAlSi$_2$O$_7$) and Fe-bearing end members [1]. Akermanite is a natural product of contact metamorphism of siliceous limestones, dolostones, and rocks of the sanidinite facies [2]. It also forms from alkalic magmas rich in calcium [2]. Gehlenite is a naturally occurring mineral in the contact zone of magma and calcite rocks [3].

Several studies on ceramics and glass-ceramics in the CaO-MgO-SiO$_2$ and CaO-MgO-Al$_2$O$_3$-SiO$_2$ system for biomedical applications have been conducted, including akermanite [4,5], merwinite [6,7], diopside [8,9], monticellite [4,10] and gehlenite [11]. Gehlenite is a common constituent of ceramic bodies, such as building ceramics and cookware [12,13]. In addition, the ceramic materials of the CaO-MgO-Al$_2$O$_3$-SiO$_2$ system are also applied as thermal barrier coating in gas turbine engines [14–16].

A variety of chemical methods, including milling [17], solid-state sintering [18], co-precipitation [19], and sol-gel synthesis [20], were used to prepare ceramics material. Wet milling is a popular method for preparing nanosuspensions. Wet milling has several advantages over dry milling, including higher energy efficiency, a lower magnitude of excess enthalpy, better heat dissipation, and the absence of dust formation due to the aqueous environment in which it is performed [21]. Besides that, there are few theories and methods to guide research on the formulation and process of wet milling. This study aimed to look into the effect of milling time on the physical and mechanical properties of ceramic derived from the CaO-MgO-Al_2O_3-SiO_2 system.

2. Methodology

The raw materials, composition, suppliers and the purity of chemicals used in this research are shown in Table 1. The powders ($7.5CaO$-$3MgO$-$3.71Al_2O_3$-$14.5SiO_2$ in weight %) were wet-milled by a planetary ball mill (Fritsch Pulverisette 6, Germany) at different milling times (30 min, 1 and 2 h) with solid to water weight ratio of 1:4. A ball to powder weight ratio of 10:1 was kept constant in the stainless steel jar. The rotational speed of the ball bill was fixed to 500 rpm. The milled ceramics slurry mixtures were dried in an oven at 85 °C for 24 h. The dried ceramics mixtures were then crushed into powder using an agate mortar. The powders were pressed at 5 tonnes to produce disc-shaped green bodies of 13 mm in diameter. The pellets were then sintered in a furnace (Carbolite, CWF1100, Germany) at 950 °C with a heating rate of 5 °C/min for a soaking time of 1 h.

Table 1 – Raw materials, compositions, suppliers and purities for fabricating ceramics powder derived from the CaO-MgO-Al_2O_3-SiO_2 system

Raw materials	Supplier	Purity
CaO	R&MI	96.0%
MgO	QReC	98.0%
Al_2O_3	Sigma Aldrich	<= 100 %
SiO_2	Sigma	99.0%

2.1 Characterisation

An X-ray diffractometer (D2 phaser, Bruker, Germany), with a step size of 0.03° and a scanning speed of 3°/min, was used to examine the phase composition of samples after milled at different times (30 min, 1 h and 2h) and sintered at 950 °C for 1 h. The linear shrinkage of the pellet samples during sintering was determined by measuring the diameter of the pellet samples before and after the sintering process with a digital calliper (Mitutoyo 150mm Digital Caliper Metric). The volume density and open porosity pellet samples were determined using the Archimedes method in distilled water using the following equations [22]:

$$Density = w_{dry}/(w_{sat} - w_{susp}) \times \rho_{liq} \quad (1)$$
$$\% porosity = (w_{sat} - w_{dry})/(w_{sat} - W_{susp}) \times 100 \quad (2)$$

Where w_{dry}, w_{sat}, w_{susp}, and ρ_{liq} refer to the pellets' dry, saturated, suspended weight and the saturating/suspending liquid density, respectively. An INSTRON 3369, with a crosshead speed of 0.5 mm/min at a load cell of 5 kN, was used to measure the compressive strength of the samples. Three samples from each group were tested to determine the average linear shrinkage, volume density, open porosity and compressive strength, and the standard deviation.

3. Results and Discussions

3.1 Particle Size

Table 2 displays the particle size and specific surface area after milling. The milling time was shown to significantly impact the particle size and specific surface area of the samples, with the particle size increasing as the milling time increased.

Table 2 - The particle size and specific surface area after the milling process

Milling time	Particle size (µm)	Specific surface area (m^2/kg)
30 min	19.1	214.7
1 h	22.8	228.9
2 h	90.8	170.6

3.2   Phase

Once the milling time was increased from 30 min to 2 h, the main phases before sintered observed were quartz (SiO_2, 98-000-5727) and magnesium calcium aluminium silicate ($Al_2Ca_{2.547}MgO_{0.453}O_{12}Si_3$, 98-002-3717). The intensity of magnesium calcium aluminium silicate peak at 34.3° was increased after 2 h milling.   After sintering at 950 °C for 1 h, the XRD patterns showed a multi-phase of quartz and akermanite-gehlenite ($Al_{0.5}Ca_2Mg_{0.75}O_7Si_{1.75}$, 98-011-1619). The intensity of quartz peak is still highest compared to akermanite-gehlenite peak for 30 min, 1 h and 2 h milling. However, after 2 h milling and sinter, the intensity of the akermanite-gehlenite phase dramatically increases, and the peak can be the dominant phase with the prolonged soaking time of sintering.

3.3   Physical Characterisation

Figure 2 shows how linear shrinkage of sintered pellet ceramics at 950°C changed as milling time increased from 30 minutes to 2 hours. The values in Fig. 2 show that the influence of shrinkage is mainly attributable to particle specific surface area. Higher specific surface area and surface energy can affect more shrinkage during thermal treatment, improving densification by decreasing porosity. Previous research looked at the effect of sintering temperature on shrinkage and revealed that sintering causes a progressive decrease in total pore surface and pore volume [23]. As a result, particle size, milling time, and sintering impacted the final product dimension.
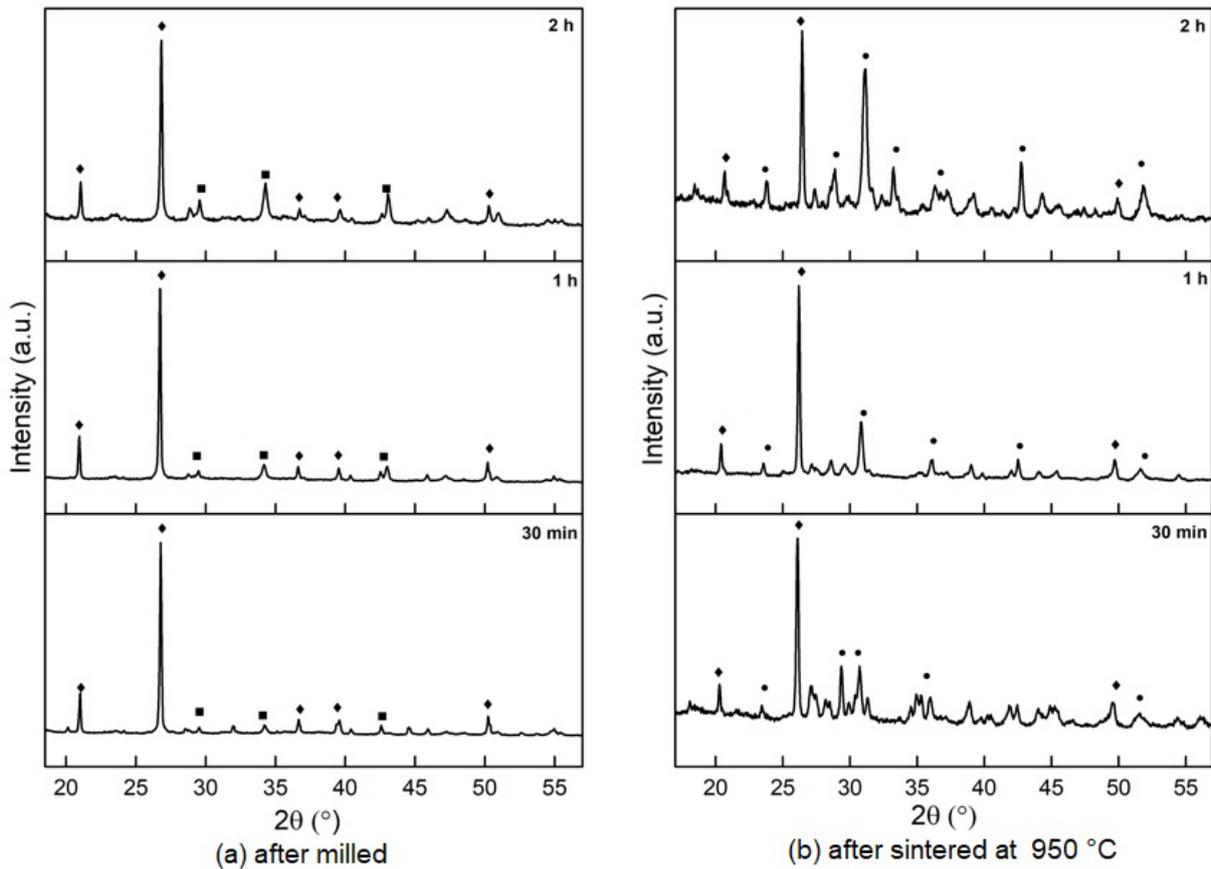

Fig. 1 - XRD patterns of the (a) milled powder for 30 min, 1 h and 2 h; (b) after sintered at 950 °C for 1 h
(◆ quartz, ■ magnesium calcium aluminium silicate and ● akermanite-gehlenite)
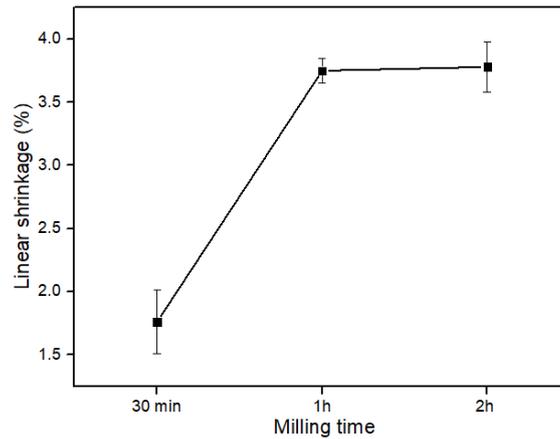
Fig. 2 - The linear shrinkage of the samples after being sintered at 950 °C and soaked for 1 h

Fig. 3 depicts the experimental densities and porosities of pellet ceramics. The results revealed that increasing the milling time causes porosities in pellet ceramics. The work hardening influence of the milling process can explain the change in porosity as milling time increases. The mixed powders are subjected to high-energy collisions between ceramic particles and milling balls during the milling process, resulting in increased powder hardness [24]. Meanwhile, particle size and the specific surface area also impact density and porosity. Whereas a small particle size results in a low specific surface area, high density value and low porosity are obtained. It can be said that the milling time did not significantly affect the densities of pellet ceramics because the difference in densities of pellet ceramics was meagre.
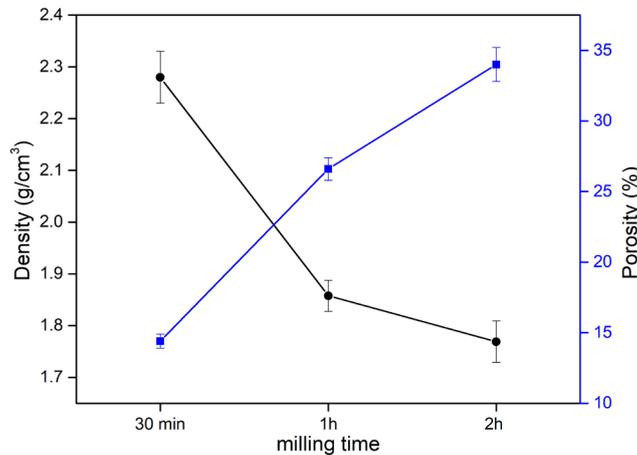

Fig. 3 - The samples' density and porosity after being milled at different times and sintered at 950 °C

3.4 Mechanical Characterisation

Compressive strength tests were performed at room temperature to evaluate ceramics' mechanical properties better, and the results are shown in Fig. 4. This software automatically calculated Young's modulus value during the compressive strength test. The highest compressive strength and Young's modulus values were 16.60 MPa and 257.09 MPa for sample 1 h milling time. The compressive strength and Young Modulus decrease with increasing the milling time. This rise can be attributed to an increase in powder hardness and a decrease in powder size. Collisions between powder particles and the ball mill during the milling process cause an increase in powder hardness. As a result of the increasing hardness of raw materials, the tensile strength of bulk samples increased. However, after 1 hour of milling, the tensile strengths decreased rapidly because increasing the ball-milling caused more work hardening, making the ceramics brittle [24]. While the highest tensile strength was obtained at the 1 h milling sample, the lowest value was obtained at the 2 h milling sample, which was 11.72 MPa. Compared to milling times of 1 h and 2 h, the tensile strength was reduced by approximately 29.4% at the end of the milling time of 2 h.
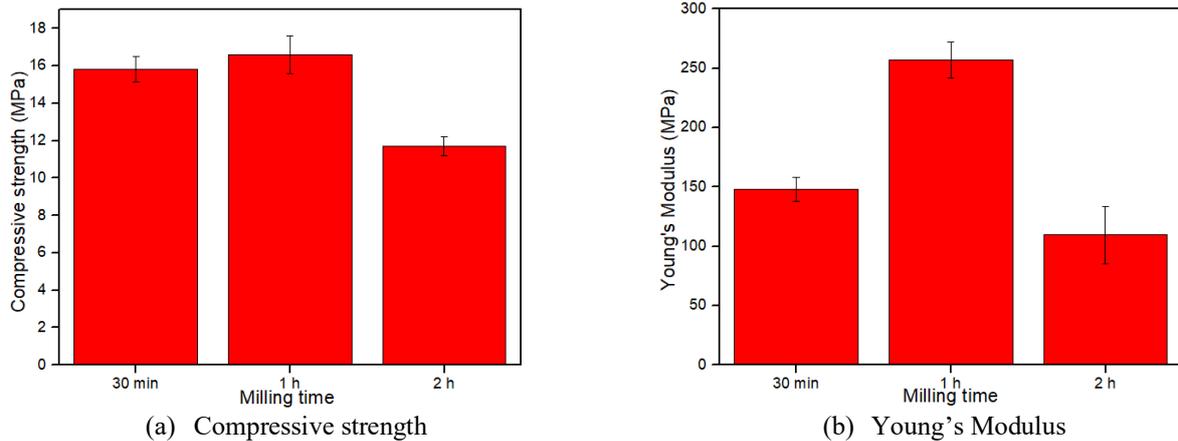
(a) Compressive strength   (b) Young's Modulus

Fig. 4 - The compressive strength and Young's modulus values of samples after milling at different times and sintered at 950 °C

4. Conclusion

Based on the results of these studies, ball milling not only causes particle size reduction or increase but may also lead to phase transitions and chemical reactions. Porosity and density measurements revealed that increasing milling time reduced density while increasing porosity. Increased milling time decreased tensile strength and Young's modulus of ceramics up to 2 hours of milling.

Acknowledgement

References

[1]   A. Amarnath, R. Dilshat, Sintering and devitrification of glass-powder compacts in the akermanite – gehlenite system, Journal of Materials Science 48, 4128–4136, 2013.

[2]   Akermanite Mineral Data, Akermanite Mineral Data (webmineral.com), 2022.

[3]   P. Ptáček, T. Opravil, F. Šoukal, J. Havlica, R. Holešinský, Kinetics and mechanism of formation of gehlenite, Al–Si spinel and anorthite from the mixture of kaolinite and calcite, Solid State Sciences, 26, 53-58, 2013.

[4]   H. Mohammadi, M. Hafezi, N. Nezafati, S. Heasarki, A. Nadernezhad, S.M.H. Ghazanfari, M. Sepantafar, Bioinorganics in bioactive calcium silicate ceramics for bone tissue repair: Bioactivity and biological properties, J. Ceram. Sci. Technol. 5, 1–12, 2014.

[5]   R. Choudhary, S. Koppala, S. Swamiappan, Bioactivity studies of calcium magnesium silicate prepared from eggshell waste by sol–gel combustion synthesis, J. Asian Ceram. Soc. 3, 173–177, 2015.

[6]   S. Praharaj, S. Kumar, R. Vasantharaman, S. Swamiappan, Sol-gel combustion synthesis of merwinite and its biomedical applications, Mater. Lett. 300, 130108, 2021.

[7]   M.S. Collin, S. Sasikumar, Effect of fuel on biomineralisation of merwinite, Mater. Lett. 304, 130660, 2021.

[8]   B.N. Sherikar, B. Sahoo, A.M. Umarji, One-step synthesis of diopside ($CaMgSi_2O_6$) ceramic powder by solution combustion method, Adv. Powder Technol. 31, 3492–3499, 2020.

[9]   M.S. Collin, S. Kumar, S. Mohana, S. Sumathi, E.A. Drweesh, M.M. Elnagar, E.S. Mosa, S. Sasikumar, Solution combustion synthesis of functional diopside , akermanite , and merwinite bioceramics : Excellent biomineralisation, mechanical strength , and antibacterial ability, Mater. Today Commun. 27, 102365, 2021.

[10]   S. Kumar, R. Choudhary, G. Krishnamurithy, H. Rao, B. Raghavendran, M. Raman, T. Kamarul, Comparative investigation on antibacterial , biological and mechanical behaviour of monticellite and diopside derived from biowaste for bone regeneration, Mater. Chem. Phys. 286, 126157, 2022.

[11]   S. Kermani, On the Bioactivity and Mechanical Properties of Gehlenite Nanobioceramic : A Comparative Study, J Med Signals Sens. 10(2), 105-111, 22020.

[12]   M. Merlini, M. Gemmi, G. Artioli, T.A. Desio, Low temperature SR-XRPD study of åkermanite-gehlenite solid solution, Z. Kristallogr. Suppl. 23, 419-424, 2006.

[13]   I. Rodica-Mariana, F. Radu-Claudiu, T. Sofia, F. Irina, B. Ioana-Raluca, Ceramic Materials Based on Clay Minerals in Cultural Heritage Study, in: Intech Open Science, 2016.

[14]   A. Nieto, M. Walock, A. Ghoshal, D. Zhu, W. Gamble, B. Barnett, M. Murugan, M. Pepi, C. Rowe, R. Pegg, Surface & Coatings Technology Layered , composite , and doped thermal barrier coatings exposed to sand laden fl ows within a gas turbine engine : Microstructural evolution , mechanical properties , and CMAS deposition, Surf. Coat. Technol. 349, 1107–1116, 2018.

[15]   A. Islam, A. Sharma, P. Singh, N. Pandit, A.K. Keshri, Plasma-sprayed CeO_2 overlay on YSZ thermal barrier coating : Solution for resisting molten CMAS infiltration, Ceram. Int. 48, 14587–14595, 2022.

[16]   R.I. Webster, E.J. Opila, Viscosity of $CaO-MgO-Al_2O_3-SiO_2$ (CMAS) melts: Experimental measurements and comparison to model calculations, Journal of Non-Crystalline Solids, 15, 121508, 2022.

[17]   H.Ismail, H. Mohamad, Preliminary Study on the Bioactivity Properties of Cordierite/β-Wollastonite Biocomposite Ceramics, Key Engineering Materials, 908, 148–153, 2022.

[18]   X. Huang, L. Zuo, X. Li, Y. Feng, X. Liu, X. Chen, Fabrication and characterisation of $Tb_3Al_5O_{12}$ magneto-optical ceramics by solid-state reactive sintering, Opt. Mater., 102, 109795, 2020.

[19]   Z. Hu, X. Chen, X. Liu, X. Li, T. Xie, Y. Shi, M. Nikl, J. Li, H. Kou, Y. Pan, E. Mih, Fabrication and scintillation properties of $Pr : Lu_3Al_5O_{12}$ transparent ceramics from co-precipitated nanopowders, Journal of Alloys and Compounds, 818, 152885, 2020.

[20]   S. Yu, W. Jing, M. Tang, T. Xu, W. Yin, B. Kang, Fabrication of Nd : YAG transparent ceramics using powders synthesised by citrate sol-gel method, J. Alloys Compd. 772, 751–759, 2019.

[21]   B.S. Meher, R. Saha, D. Chaira, Fabrication of MWCNTs reinforced iron metal matrix composite by powder metallurgy_ Effects of wet and dry milling, J. Alloys Compd. 872, 159688, 2021.

[22]   M.S.K. Mubina, S. Shailajha, R. Sankaranarayanan, L. Saranya, In vitro bioactivity, mechanical behavior and antibacterial properties of mesoporous $SiO_2-CaO-Na_2O-P_2O_5$ nano bioactive glass ceramics, J. Mech. Behav. Biomed. Mater. 100, 103379, 2019.

[23]   I. Cristofolini, A. Rao, C. Menapace, A. Molinari, Influence of sintering temperature on the shrinkage and geometrical characteristics of steel parts produced by powder metallurgy, J. Mater. Process. Tech. 210, 1716–1725, 2010.

[24]   M. Çelebi, A. Çanakçi, S. Özkaya, A.H. Karabacak, The Effect of Milling Time on the Mechanical Properties of ZA_{27}/Al_2O_3 Nanocomposites, 6, 163–169, 2018.